Phase stability of multicomponent NAPLs containing PAHs

ARTICLE *in* ENVIRONMENTAL SCIENCE AND TECHNOLOGY · AUGUST 1997

Impact Factor: 5.33 · DOI: 10.1021/es960948m

4 AUTHORS, INCLUDING:

Catherine A. Peters
Princeton University
96 PUBLICATIONS **2,158** CITATIONS
SEE PROFILE

Suparna Mukherji
Indian Institute of Technology Bombay
68 PUBLICATIONS **1,506** CITATIONS
SEE PROFILE

Christopher D Knightes
United States Environmental Protection Age…
38 PUBLICATIONS **529** CITATIONS
SEE PROFILE

Phase Stability of Multicomponent NAPLs Containing PAHs

CATHERINE A. PETERS,*,† SUPARNA MUKHERJI,‡ CHRISTOPHER D. KNIGHTES,† AND WALTER J. WEBER, JR.‡

Department of Civil Engineering and Operations Research, Princeton University, Princeton, New Jersey 08544, and Department of Civil and Environmental Engineering, The University of Michigan, Ann Arbor, Michigan 48109-2125

Multicomponent nonaqueous phase liquid (NAPL) contaminants that contain compounds that are solids in their pure states can undergo phase transformations. This paper examines the relationship between NAPL composition and liquid phase stability for mixtures of polycyclic aromatic hydrocarbons (PAHs), most of which are solids in pure form at ambient temperatures. Because any natural or engineered process that acts to selectively extract compounds will alter NAPL composition, knowledge of phase stability is an important determinant in risk assessment, remediation effectiveness, and research. Ideal solubility theory dictates that a NAPL will be a homogeneous liquid if each constituent's mole fraction is less than the solid−liquid reference fugacity ratio at the system temperature. Through experimental observation of binary and ternary systems, it is shown that ideal solubility theory is a reliable guide for predicting PAH−NAPL phase stability. Uncertainty in melting temperature and entropy of fusion is a significant determinant that may limit predictive power. The principle of liquefaction through mixing was exploited to produce complex synthetic NAPLs which can be used as surrogate materials to simulate the behavior of contaminants such as coal tars. NAPL/aqueous phase equilibrium studies were conducted to demonstrate the utility of these materials in experimentation.

Introduction

Many organic contaminants are complex, multicomponent mixtures that are present in the environment as separate organic liquid phases, commonly referred to as nonaqueous phase liquids (NAPLs). Those that are derived from petroleum or coal processing have some fraction of aromatic hydrocarbons, which may pose a risk to human health. An example is coal tar, which is a dense NAPL consisting primarily of polycyclic aromatic hydrocarbons (PAHs), that commonly exists as a subsurface environmental contaminant at sites of former manufactured gas plants (*1*).

Multicomponent NAPLs containing PAHs can exist as liquids even though most PAHs are solids in their pure form at ambient temperatures. Melting point depressions can result for all constituent compounds because PAH mixtures form eutectic systems. The larger the number of constituent compounds, the larger is the window of possible system compositions that are stable liquid solutions at ambient temperatures. Processes that alter NAPL phase composition can result in transformation to solid. The dissolution and partitioning behavior of a contaminant is dependent on its phase state. For solid phase contaminants in contact with water, the maximum aqueous phase concentration is determined solely by the solute aqueous solubility. For multicomponent organic liquid contaminants, the maximum aqueous phase concentration of a constituent depends on its NAPL phase mole fraction, NAPL phase activity coefficient, and pure subcooled liquid solubility. Consequently, knowledge of NAPL phase stability and the possibility for phase transitions is important for risk assessment, predicting remediation effectiveness, and experimental research.

In this paper, we discuss NAPL/solid/aqueous phase equilibria and discuss predictive thermodynamic relations that describe solubility limits for NAPL constituents. We demonstrate how these constraints extend to multicomponent systems and explore the utility of these relations in providing composition criteria for phase stability of multicomponent NAPLs containing PAHs. An experimental investigation of solid−liquid phase equilibria was conducted for simple binary and ternary systems. Experimental results demonstrate the extent to which ideal solubility estimates, using melting temperature and entropy of fusion data from the literature, predict solubility limits in the NAPL. The effect of uncertainty in predictive parameters was assessed using first-order analysis. Analysis of published coal tar composition data demonstrates that these principles hold for very complex mixtures.

Also, we have employed the principles of liquefaction through mixing to enable controlled laboratory study of NAPLs that are PAH mixtures. Experimental investigations involving complex multicomponent NAPLs are often limited by the analytical difficulties that preclude complete characterization of composition and bulk properties, making it difficult to draw inferences from experimental data. We describe a procedure to generate a synthetic PAH-containing NAPL for which the complete composition is readily determined. This synthetic NAPL can be used as a model organic liquid that is representative of materials such as coal tar, without involving the uncertainties associated with field samples. In this paper, NAPL/aqueous phase equilibrium studies are presented to demonstrate the utility of this material for experiments to simulate PAH−NAPL contamination in aqueous environments and to demonstrate the thermodynamic criteria for the liquid phase stability of multicomponent NAPLs.

Multicomponent NAPL Stability and Phase Equilibria

NAPL/Solid Systems. Thermodynamic theory of phase equilibria dictates the equality of fugacities for components across phases. For a solid PAH in equilibrium with a multicomponent NAPL, assuming that the fugacity of the solute in the solid is equivalent to that of pure solid *i*, the requisite equality of fugacities for compound *i* is written

$$f^{s}_{p,i} = x_i^N \gamma_i^N f^{l}_{p,i} \quad (1)$$

where x_i^N is the mole fraction of *i* in the NAPL phase, γ_i^N is its activity coefficient in the NAPL phase, $f^{l}_{p,i}$ is the reference fugacity of pure liquid *i*, and $f^{s}_{p,i}$ is the reference fugacity of pure solid *i*. For compounds that are solids in the pure state at the system temperature, $f^{l}_{p,i}$ refers to a hypothetical subcooled liquid state. In notation from here on the subscript

* To whom correspondence should be addressed. E-mail: cap@princeton.edu; Telephone: (609)258-5645; fax: (609)258-2799.
† Princeton University,
‡ The University of Michigan.

S0013-936X(96)00948-0 CCC: $14.00

p is implied. Equation 1 rearranges to provide the inequality

$$x_i^{\mathrm{N}} \leq \frac{1}{\gamma_i^{\mathrm{N}}}\left(\frac{f^{\mathrm{s}}}{f^{\mathrm{l}}}\right)_i \tag{2}$$

representing the solubility limit of *i* in the NAPL phase.

The liquid−solid fugacity ratio ($f^{\mathrm{l}}/f^{\mathrm{s}}$) is indicative of the Gibbs energy needed to convert solid *i* to liquid *i*, at a particular temperature. Hildebrand and Scott (*2*), and more recently Prausnitz et al. (*3*), demonstrated that a compound's fugacity ratio can be calculated using

$$\ln \frac{f^{\mathrm{l}}}{f^{\mathrm{s}}} = \frac{\Delta h^{\mathrm{f}}}{RT_{\mathrm{m}}}\left(\frac{T_{\mathrm{m}}}{T} - 1\right) \tag{3}$$

where Δh^{f} is the enthalpy of fusion at the melting temperature (T_{m}), T is the system temperature, and R is the universal gas constant. Derivation of eq 3 requires assumptions that the compound's melting temperature is approximately equal to its triple point and the heat capacities of solid and liquid *i* are approximately equal. Melting temperatures are fairly easy to measure, and numerous observations have been reported in the literature for PAHs. The enthalpy of fusion is more difficult to measure, and fewer values have been reported for PAHs. Where data are unavailable, Δh^{f} can be approximated from $\Delta h^{\mathrm{f}} = T_{\mathrm{m}}\Delta s^{\mathrm{f}}$, where a common value for Δs^{f}, the entropy of fusion at the melting temperature, is assumed. Yalkowsky (*4*) demonstrated that for rigid molecules the entropy of fusion is roughly constant with a median value of 13.5 cal/mol-K. This approximation method is commonly used for data compilations such as Mackay et al. (*5*).

The constraint given in eq 2 illustrates that the solubility limit for x_i^{N} is dependent on the composition of the NAPL (i.e., the mole fractions of other constituent compounds) entirely through the γ_i^{N} term. If the NAPL is an ideal solvent for compound *i*, i.e., $\gamma_i^{\mathrm{N}} \approx 1$, then eq 2 simply states that the NAPL phase mole fraction cannot exceed the solid−liquid fugacity ratio. In this case, the solubility limit for x_i^{N} is an inherent property of the compound, referred to as its ideal solubility (*3*). The same constraint would apply for the solubility of *i* in any organic liquid that behaves as an ideal solvent. The assumption of ideality in the NAPL phase (Raoult's law) implies that the molecular interactions of a constituent in the NAPL solution are the same as for that compound in a liquid of pure material. Because of the chemical similarity of constituent compounds, Raoult's law is usually a reasonable approximation for PAH-containing NAPLs. Recent experimental work has shown that the assumption of ideality holds for these mixtures (*6*).

Very little information on solid−liquid phase equilibria for PAHs has been published. Rudolfi (*7*) published experimental observations for binary naphthalene/phenanthrene and naphthalene/anthracene systems, demonstrating eutectic systems with good agreement between experimental and ideal solubilities. Their observations also validate the assumption of pure solid formation, which is implicit in eq 1.

NAPL/Aqueous Phase Systems. When a multicomponent NAPL is in equilibrium with water, the requisite equality of fugacities results in the following relation for the equilibrium aqueous phase concentration, C_i^{A} (mg/L), of a NAPL phase constituent:

$$C_i^{\mathrm{A}} = x_i^{\mathrm{N}}\gamma_i^{\mathrm{N}}C_{\mathrm{s},i}\left(\frac{f^{\mathrm{l}}}{f^{\mathrm{s}}}\right)_i \tag{4}$$

where $C_{\mathrm{s},i}$ is the aqueous solubility of pure *i* (mg/L). The product of $C_{\mathrm{s},i}$ and $(f^{\mathrm{l}}/f^{\mathrm{s}})_i$ is the pure solute subcooled liquid solubility. Derivation of eq 4 and its implicit assumptions has been previously discussed (*8*), and similar theoretical discussions have been put forth by others in various contexts (e.g., refs 9−15).

TABLE 1. Demonstration of NAPL Phase Stability Criterion for Field Samples of Tar Materials

		x_i^{N}, mole fraction[a]		
	mol wt	site 4 liquid tar	site 6 solid tar	$(f^{\mathrm{s}}/f^{\mathrm{l}})^b$ 25 °C
benzene	78	1.2e-5	2.2e-4	1.0
toluene	92	1.3e-4	ND[c]	1.0
ethylbenzene	106	6.5e-4	ND	1.0
o-xylene	106	0.0011	3.0e-5	1.0
m/*p*-xylenes	106	0.0040	ND	1.0
indan	118	8.0e-4	ND	1.0
naphthalene	128	0.0934	0.0121	0.30
1-methylnaphthalene	142	0.0348	0.0072	1.0
2-methylnaphthalene	142	0.0606	0.0079	0.86
acenaphthylene	152	0.0183	0.0094	0.22
acenaphthene	154	0.0013	0.0048	0.20
dibenzofuran	168	0.0015	0.0176	0.25
fluorene	166	0.0095	0.0137	0.16
anthracene	178	0.0070	0.0268	0.0098
phenanthrene	178	0.0220	0.1020	0.27
fluoranthene	202	0.0054	0.0675	0.19
pyrene	202	0.0078	0.0489	0.13
benz[*a*]anthracene	228	0.0024	0.0135	0.04
chrysene	228	0.0024	0.0166	0.0097
benzo[*b*]fluoranthene	252	0.012	0.0098	0.039
benzo[*k*]fluoranthene	252	5.6e-4	0.0053	0.013
benzo[a]pyrene	252	0.014	0.0090	0.03
indeno[1,2,3-*cd*]pyrene	276	9.0e-4	0.0203	0.04
dibenz[*a*,*h*]anthracene	278	1.2e-4	0.0026	0.004
benzo[*g*,*h*,*i*]perylene	276	0.011	0.0241	0.003

[a] Computed using data published in EPRI (*18*). [b] Computed using data published in Daubert and Danner (*19*) where available; otherwise from Mackay et al. (*5*). [c] Nondetectable.

When a solid PAH is in equilibrium with water, we have by definition $C_i^{\mathrm{A}} = C_{\mathrm{s},i}$. Substituting the right-hand side of the inequality in eq 2 for x_i^{N} in eq 4, we see that $C_{\mathrm{s},i}$ serves as the upper limit for the concentration in the aqueous phase for a system in which a multicomponent NAPL is in equilibrium with water.

Implications for NAPL Aging. The thermodynamic constraint on NAPL phase mole fractions shown in eq 2 has implications for the natural weathering of NAPL contaminants over time in saturated subsurface environments and for accelerated weathering effected by pump-and-treat remediation processes. As lower molecular weight, more soluble compounds are extracted from a multicomponent NAPL, the mole fractions of the higher molecular weight compounds increase. Eventually, as compound mole fractions reach their solubility limits in the NAPL phase, portions of the NAPL will precipitate out and form solid. In other papers, we present numerical simulations of NAPL composition dynamics and the resulting impact on NAPL phase behavior and dissolution (*16*, *17*).

To demonstrate the NAPL phase stability concept for contaminants in the field, published coal tar composition data are shown in Table 1 for two tar materials (*18*). Raoult's law has been assumed for the present demonstration. The liquid tar material from site 4 has a composition for which the mole fractions do not violate the constraint given in eq 2. In contrast, the tar material from site 6 is described as a hard solid. Several violations of the constraint in eq 2 are observed in the composition data for this tar, specifically for anthracene, chrysene, and benzo[*g*,*h*,*i*]perylene. Violation of the constraint in eq 2 is more likely for the higher molecular weight compounds, and additional violations are likely to occur for the higher molecular weight compounds that are not specifically identified in the composition analysis for the site 6 tar.

TABLE 2. Physical and Chemical Properties of Compounds Used in Experimental Systems

compound	mol wt	melting point[a] (°C)	Δs^f at T_m[a] (cal mol^{-1} K^{-1})	f^s/f^l 25 °C	$C_{s,i}$[b] (mg/L) 25 °C
toluene	92.14	−95	8.90	1	530
naphthalene	128.17	80	12.83	0.30 (±0.10)	31
1-methylnaphthalene	142.20	−30	6.84	1	28
2-methylnaphthalene	142.20	35	9.42	0.86 (±0.06)	25
2-ethylnaphthalene	156.23	−4	13.5	1	8
acenaphthene	154.21	93	13.99	0.20 (±0.80)	3.8
fluorene	166.22	115	12.06	0.16 (±0.09)	1.9
phenanthrene	178.23	99	10.57	0.27 (±0.12)	1.1
fluoranthene	202.26	110	11.68	0.19 (±0.09)	0.26
pyrene	202.26	151	9.79	0.13 (±0.09)	0.13

[a] Source: Daubert and Danner (*19*). Entropies of fusion were computed from reported enthalpies of fusion and melting temperatures. [b] Based on data compiled by Mackay et al. (*5*).

In the remainder of the paper, we present experimental observations of phase stability of binary and ternary PAH mixtures, formulations of more complex PAH−NAPLs, and phase equilibria of multicomponent NAPL/aqueous phase systems. The validity of the conditionality shown in eq 2 as a predictor of NAPL phase stability together with its associated uncertainty is demonstrated.

Materials and Methods

Chemicals. PAHs used in this study were obtained from Aldrich Chemical Co. and had a purity greater than or equal to 97%. The reported purities of the compounds for which freezing point observations were made are 99+% for naphthalene, 98% for 2-methylnaphthalene, and 99+% for 2-ethylnaphthalene. HPLC-grade toluene, acetonitrile, and methanol were obtained from Mallinckrodt, Inc. The water used was double-distilled, deionized water (Milli-Q, Millipore Corp.). Prepurified nitrogen used for purging the NAPL in its preparatory stages had a purity of 99.98%. All reagents were used as received.

Binary Solid−Liquid Phase Equilibria. Three binary pairs were examined using naphthalene, 2-methylnaphthalene, and 2-ethylnaphthalene. Binary mixtures of specific compositions were prepared in sealed vials by weighing desired amounts of each compound to sum to a total mass of approximately 5 g. For each binary pair, 11 mixtures were prepared in increments of tenths of mole fraction.

Each vial was heated until the contents formed a homogeneous liquid phase, and then solidified by cooling to −15 °C. Freezing point determinations followed three similar protocols depending on freezing points: (a) 20 °C and up, (b) 8−20 °C, and (c) below 8 °C. According to this breakdown, each vial was placed in (a) a water bath on a heating mantle, (b) an ice and water bath, or (c) a methanol−water solution bath submerged in dry ice. The samples were heated slowly (i.e., < 0.2 °C/min). Visual observation indicated the temperature at which the sample was completely liquefied. Freezing points were not determined by cooling because of the tendency to form subcooled liquids that would suddenly crystallize at lower temperatures. For each vial, three replicate observations were made, which resulted in standard deviations of less than 1 °C.

Ternary Solid−Liquid Phase Equilibria. One ternary system was examined consisting of naphthalene, acenaphthene, and 2-methylnaphthalene. Solid−liquid phase equilibria observations were made at a single temperature by determining the boundaries of the two-phase regions of the ternary phase diagram. For naphthalene and acenaphthene phase boundaries, individual experimental systems were prepared with overall compositions within the two-phase regions. The chemicals were added to individual centrifuge tubes, which were then sealed and heated to liquefy. The vials were then cooled to the system temperature, 26 ± 1 °C, by equilibration in a constant temperature room for 1 day. The vials were centrifuged (10 min at 430*g*), and the liquid phase was sampled and analyzed using HPLC techniques for NAPL samples as described below.

For 2-methylnaphthalene, it was not possible to design experiments with overall system compositions that resulted in two-phase systems with a sufficiently large volume of liquid phase for sampling. This phase boundary was determined by successive bracketing. Systems with overall compositions near and around the phase boundary were prepared. After equilibration, visual inspection determined whether the composition resulted in a two-phase or homogeneous liquid system. By averaging the mole fractions of proximal liquid systems and two-phase systems, bisection points were determined which had associated uncertainties of less than ±0.02 mole fraction units.

Synthetic NAPL Preparation. Several complex multicomponent synthetic NAPLs were prepared from eight PAHs that are common coal tar constituents: naphthalene, 1-methylnaphthalene, 2-ethylnaphthalene, acenaphthene, fluorene, phenanthrene, fluoranthene, and pyrene. Table 2 lists the physical and chemical properties of these compounds. The initial relative amounts of PAHs were chosen such that the mole fractions would not exceed the corresponding fugacity ratios at 25 °C.

The procedure for making the synthetic NAPLs involves dissolution of predetermined amounts of the PAHs in toluene and subsequent evaporation of the bulk of the toluene. Toluene was chosen because of its high PAH solubility so as to minimize solvent requirements, its high volatility so as to facilitate separation from the resulting NAPL, and its aromatic nature such that residual solvent would not affect the aromatic character of the resulting NAPL. Removal of toluene was achieved first through rotary evaporation (Bucchi Rotovapor Model R-110) at 50 °C for 3 h, which reduced the toluene mole fraction to about 0.5. Residual toluene was removed by nitrogen purging for several days until the NAPL volume was constant, which corresponded to a toluene mole fraction of less than 0.05. The final NAPL density was denser than water. The resulting NAPL composition was determined using HPLC analysis.

Four synthetic NAPLs were prepared: two with naphthalene and two without naphthalene. All were prepared initially without naphthalene, and this compound was added subsequently when desired by direct dissolution of a measured mass of crystals. Heating in a water bath aided the dissolution of naphthalene. The naphthalene concentration in the synthetic NAPLs could thus be controlled as a design variable for subsequent experiments.

Batch Equilibration Experiments. NAPL/aqueous phase equilibrium experiments were conducted in 25-mL corex glass high-speed centrifuge tubes containing approximately 0.5 g of NAPL and 25 mL of Milli-Q water. The tubes were sealed

and tumbled end-over-end in the dark for 2 weeks at 25 °C. Following equilibration, phase separation was aided by centrifugation at 7500 rpm for 30 min (Sorvall Centrifuge Model RC-5B, Dupont, Inc.). The aqueous phase was sampled and analyzed immediately. The NAPL phase was sampled, diluted in methanol (dilution factor 1000), transferred into autosampler vials, and stored at 5 °C prior to analysis.

HPLC Analysis. The concentrations of all compounds in the NAPL and the aqueous phases were analyzed using a Hewlett Packard 1090 high-performance liquid chromatograph (HPLC) equipped with a diode array UV detector (DAD) and a fluorescence detector (FLD). A reverse-phase octadecylsilane column with 5 μm packing diameter and dimensions of 250 mm by 4.6 mm (VYDAC 201 TP, The Separations Group, Hesperia, CA) was used. The chromatography program was as follows: flow rate of 1 mL/min, at 35 °C, 50% acetonitrile for 5 min, rising with a linear gradient to 65% acetonitrile at 30 min, remaining constant at 65% up to 33 min, post time of 5 min, injection volume of 5 μL for NAPL samples and 15 μL for aqueous samples. Calibration curves bracketing the range of expected unknown concentrations were generated using external standard solutions containing all of the compounds dissolved in methanol. Duplicate injections were made for each standard and sample. Only the DAD detector (at 220 and 240 nm) was used for quantification of PAHs in the NAPL phase diluted in methanol. Both the DAD detector and the FLD detector were used for quantification of PAHs in aqueous samples. The FLD detector was set at 220 Hz and was time-programmed with respect to PMT gain and wavelengths for excitation and emission.

Results and Discussion

Ideal Solubility Predictions and Uncertainty Analysis. For each compound, ideal solubilities were estimated using fugacity ratios calculated from eq 3, with the melting temperatures and entropies of fusion reported in Daubert and Danner (*19*). Fugacity ratios at 25 °C, expressed in the common form of (f^s/f^l), are shown in Table 2. For 2-ethylnaphthalene, neither a reliable value of Δs^f nor T_m is available, so $\Delta s^f = 13.5$ cal/mol-K was assumed (*4*), and the experimental observation for T_m from this study was used. Examination of Table 2 reveals that the values of Δs^f do not all fall within the 10−17 cal/mol-K range theorized for rigid molecules (*4*) and that appreciable errors would result if the common value of 13.5 was assumed to hold for all PAHs. Differences in fugacity ratios across compounds arise mainly from the magnitude of T_m/T. For higher molecular weight PAHs, with very high melting points, the value of (f^s/f^l) becomes very small.

An uncertainty analysis was conducted to estimate the uncertainty in ideal solubility predictions and the extent to which it is attributable to uncertainty in T_m and Δs^f. This was accomplished using a first-order approximation for variance in a derived variable (*20*), which assumes independent errors, negligible covariances, and negligible higher order effects. This, combined with differentiation of eq 3, results in

$$\sigma^2_{\ln f^l/f^s} \cong \sigma^2_{T_m}\left(\frac{\Delta s^f}{RT}\right)^2 + \sigma^2_{\Delta s^f}\frac{1}{R^2}\left(\frac{T_m}{T}-1\right)^2 \qquad (5)$$

where σ_x^2 is the variance of variable x. Based on the ranges of values reported for melting temperatures of PAHs (*5*), σ_{T_m} was estimated to be 2 °C. Because little published data exist for enthalpies of fusion of PAHs, the associated uncertainties are difficult to estimate. It is assumed that $\sigma_{\Delta s^f}$ is 3.5 cal/mol-K, which is taken from the range of Δs^f for rigid molecules reported to be 10−17 cal/mol-K (*4*). Because γ_i^N is assumed to equal unity in an ideal solubility prediction, eq 5 also represents the relative variance of the mole fraction solubility limit, $(\sigma_{x_i^N}/x_i^N)^2$. The resulting 1σ error estimates for fugacity ratio are shown in Table 2. Relative errors range from 6% for 2-methylnaphthalene to 70% for pyrene, revealing that the uncertainty increases as the ratio of T_m/T becomes large.

Binary Solid−Liquid Phase Equilibria. For each of the three binary pairs, freezing point curves were computed through estimation of ideal solubilities as a function of system temperature and are shown in Figure 1. In binary temperature−composition diagrams, these curves separate homogeneous liquid systems (above) from systems that are two-phase or homogeneous solids (below). In all three binary systems studied, the assumption of ideality predicts a eutectic point where the ideal solubility curves intersect, below which no liquid phase is stable. The implication of this type of binary solid/liquid phase diagram is that for temperatures below the melting temperatures of both components, there is a window of viable compositions for which mixtures will exist as homogeneous liquids. For example, for naphthalene and 2-methylnaphthalene, ideal solubility theory predicts that at 25 °C homogeneous liquid systems will exist for mixtures with compositions having a 2-methylnaphthalene mole fraction greater than 0.70 and less than 0.86. Systems with naphthalene mole fractions greater than 0.30 at 25 °C would contain solid naphthalene in equilibrium with a binary liquid solution containing naphthalene at its solubility limit. Similarly, at the other phase boundary solid 2-methylnaphthalene would form.

The dotted curves depict the range of uncertainty in the solubility limits at a given temperature. In the limit of $x_i \rightarrow 1$, the uncertainty in the solubility limit approaches a limiting value of $\sigma_{T_m}\Delta s^f/(RT)$, which is due solely to uncertainty in the melting temperature. As the system temperature becomes different from T_m, the ideal solubility estimate is increasingly sensitive to the uncertainty in Δs^f. For example, at 25 °C the solubility limit for naphthalene of 0.30 has an uncertainty of ±0.10, of which 98% is due to uncertainty in Δs^f.

Also shown in Figure 1 are the experimental observations. Observed melting temperatures for the pure systems are 80.6 °C for naphthalene, 34.0 °C for 2-methylnaphthalene, and −4.4 °C for 2-ethylnaphthalene. The first two values are in close agreement with literature reported values (Table 2). Close agreement with ideal solubility theory is shown for the binary systems except near the eutectic points for the two systems containing 2-methylnaphthalene. The deviations observed for the solubility limit of 2-methylnaphthalene may be explained by uncertainty in Δs^f, but as is discussed below, the results from the ternary system analysis indicate some NAPL phase nonideal behavior for 2-methylnaphthalene.

Ternary Solid−Liquid Phase Equilibria. The solid−liquid phase diagram for the ternary system containing naphthalene, 2-methylnaphthalene, and acenaphthene at 26 °C is shown in Figure 2. The solid lines delineate the two-dimensional space bounding the window of viable compositions of mixtures that will exist as homogeneous liquids, as predicted by ideal solubility theory. At 26 °C homogeneous liquid systems will exist for mixtures of these three compounds provided that naphthalene's mole fraction is less than 0.31, 2-methylnaphthalene's mole fraction is less than 0.87, and acenaphthene's mole fraction is less than 0.20. Overall system compositions outside of this region will result in multiphase systems. The effect of increases in temperature on the ternary solid−liquid phase diagram would be enlargement of the window of compositions forming homogeneous liquids.

Experimental observations of the liquid phase compositions are shown in Figure 2 as open symbols. For naphthalene and acenaphthene, the experimentally determined solubility limits are slightly but consistently lower than those predicted by ideal solubility theory. For 2-methylnaphthalene, the experimentally observed solubility limit is lower than the ideal prediction when the mixture is rich in naphthalene and higher when the mixture is rich in acenaphthene. The deviations observed in the ternary phase diagram for the naphthalene/

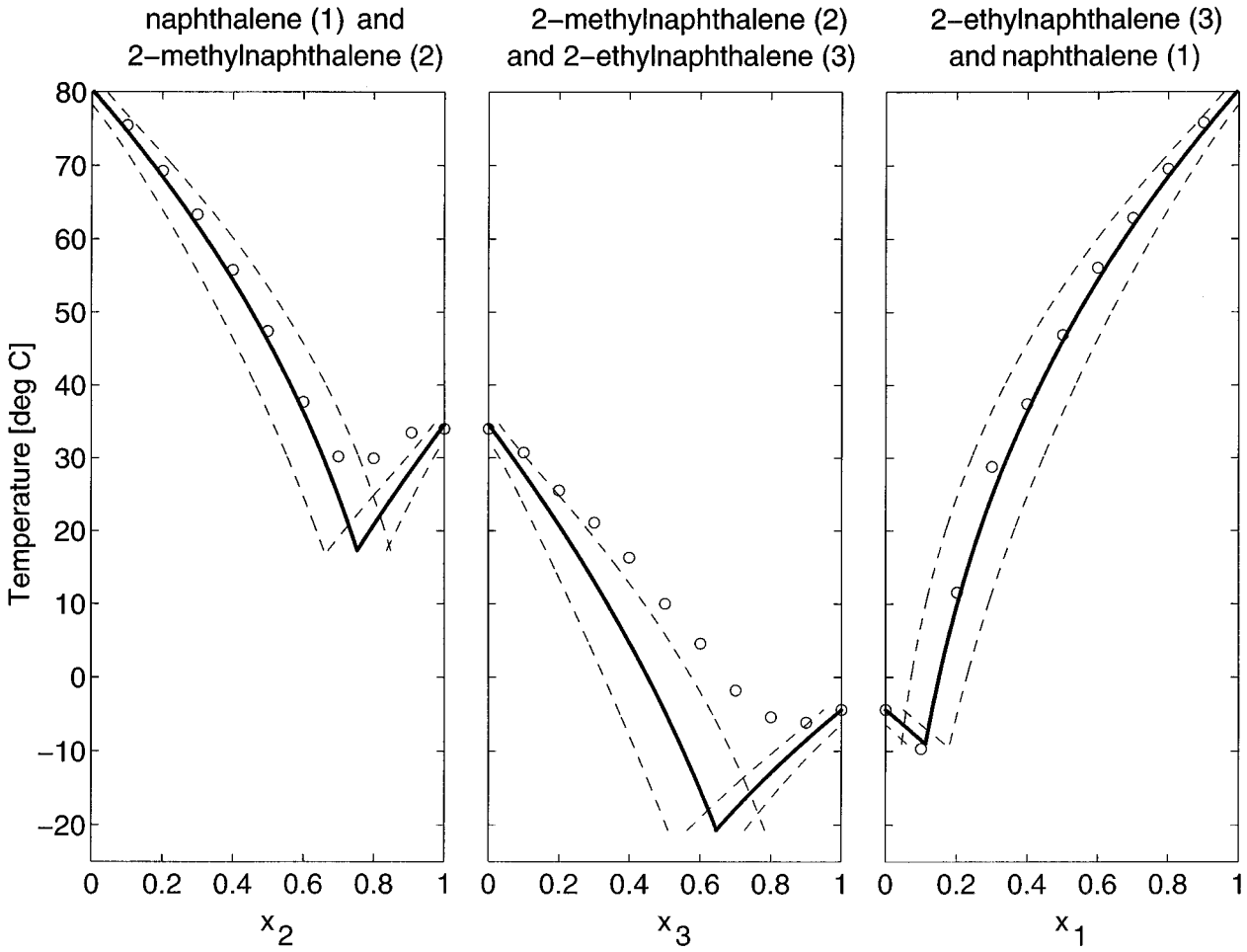

FIGURE 1. Temperature–composition diagrams of solid–liquid equilibria for three binary PAH mixtures. Circles are experimental observations. Solid curves are the ideal solubility predictions, and dotted curves bound the associated uncertainty in these predictions.

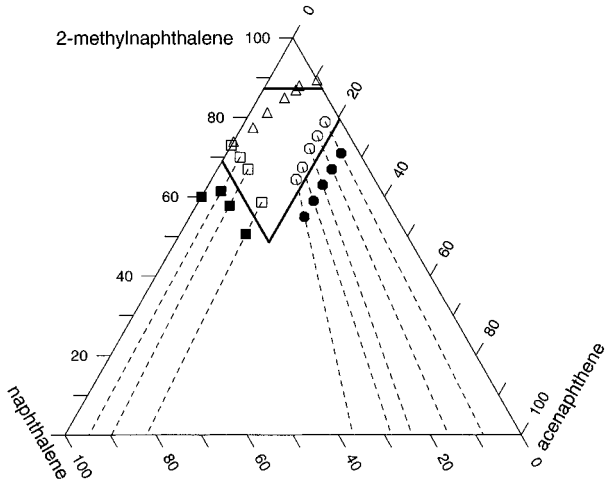

FIGURE 2. Solid–liquid phase diagram for ternary PAH mixture at 25 °C. Open symbols are experimental observations of liquid phase composition boundaries. Dashed lines represent experimental tie line observations. Solid lines denote ideal solubility limits.

2-methylnaphthalene binary pair are consistent with those observed at 26 °C in the binary system depicted in Figure 1. Uncertainty bands for the ideal solubility limits are not shown in the diagram, but can be inferred from the estimated errors in the fugacity limits listed in Table 2. If it is assumed that the fugacity ratios have been accurately estimated, deviation of experimental observations may be an indication of nonideality in the NAPL phase. For 2-methylnaphthalene, because the observed solubility limit curve is nonparallel with the ideal solubility limit, deviation cannot be explained by uncertainty in the fugacity ratio. It was observed that a binary mixture of naphthalene and 2-methylnaphthalene has a solubility limit of 0.74 mole fraction for 2-methylnaphthalene, corresponding to $\gamma_i^N = 1.2$. For a binary mixture of acenaphthene and 2-methylnaphthalene, the mole fraction limit for 2-methylnaphthalene is 0.89, corresponding to $\gamma_i^N = 0.98$.

Regardless of whether observed deviations indicate slight deviations from ideality or uncertainty in the parameters used to predict fugacity ratios, these results indicate that for all three compounds in the ternary system the ideal solubility predictions provide a reliable means of estimating the window of NAPL phase stability. The valid use of eq 1 to predict solid–liquid phase equilibria for systems within the multiphase region is less clear. Ideal solubility theory predicts that an overall composition that violates only one solubility constraint would consist of a two-phase system: a liquid solution and a solid solution rich in the compound whose solubility constraint is violated. Tie lines would connect the points, indicating the compositions of these two phases. A system with an overall composition that violates two of the solubility constraints would result in a three-phase system of liquid solution and two solids nearly pure in each of the two compounds. For example, according to ideal solubility theory, a mixture that has a naphthalene mole fraction exceeding 0.31 and an acenaphthene mole fraction exceeding 0.20 would produce a liquid phase of 0.31 mole fraction naphthalene, 0.20 mole fraction acenaphthene, and 0.49 mole fraction 2-methylnaphthalene. This liquid phase would be in equilibrium with two solids, one rich in naphthalene and one rich

TABLE 3. Composition and Property Data for Four Synthetic PAH−NAPLs

	x_i^N, mole fraction			
compound	NAPL1	NAPL2	NAPL3	NAPL4
toluene	ND	ND	0.021	0.018
naphthalene		0.297		0.116
1-methylnaphthalene	0.214	0.233	0.301	0.266
2-ethylnaphthalene	0.094	0.056	0.146	0.129
acenaphthene	0.203	0.121	0.155	0.137
fluorene	0.087	0.053	0.067	0.060
phenanthrene	0.175	0.104	0.135	0.119
fluoranthene	0.153	0.091	0.117	0.104
pyrene	0.074	0.044	0.058	0.051
rel. error in x_i^N	<1%	1%	4%	<1%
mol wt	168	153	162	158
density (g/mL) (25 °C)	1.09	1.08	1.07	1.10

in acenaphthene. The exact proportions of the three phases would be determined by the lever rule (*21*).

The formation of solid solutions is evidenced in Figure 2 by the slopes of the observed tie lines which connect liquid phase compositions with overall system compositions shown as filled symbols. Solid phase compositions were not determined, but for each system the solid phase composition lies somewhere along the tie line. The three systems that exceed the naphthalene solubility limit and the five systems that exceed the acenaphthene solubility limit all result in the formation of solid of both naphthalene and acenaphthene.

Synthetic NAPL Formulations. Table 3 lists the mole fractions of the components and bulk properties for each of the four synthetic NAPLs. The mole fractions are based on measurements of concentration in the NAPL phases after equilibration with water and, based on mass balance considerations, are very similar to the mole fractions prior to equilibration. Density was computed by summing the mass concentrations of the NAPL phase constituents, which assumes that the composition is completely characterized. In an analogous fashion, the reciprocal of the molar volume was computed using molar concentrations. The number-average molecular weight was then computed as the product of NAPL density and molar volume.

NAPLs 1 and 2 were the first formulations to be made that were homogeneous liquids at ambient conditions, but when the temperature in the laboratory dropped below 20 °C, a solid precipitate was observed. When warmer conditions returned, the solid dissolved, thus indicating a reversible temperature-dependent solid−liquid phase equilibrium. In an effort to produce a more stable synthetic NAPL, the system was forced through a phase transition by a cycle of cooling to 15 °C, removal of the solid phase, and rewarming to 25 °C. After NAPL 1 was put through this cycle, the resulting liquid phase contained higher mole fractions of 1-methylnaphthalene, 2-ethylnaphthalene, and fluorene. The liquid phase composition after cooling was used to design NAPL 3. Both NAPLs 3 and 4 were stable for temperatures approximately above 10 °C.

These efforts demonstrate the ability to design multicomponent PAH formulations that result in homogeneous liquid phases and are stable with respect to temperature variations. This extends the results from the binary and ternary systems to further validate the contention that ideal solubility limits can serve as useful guides for prediction of NAPL phase stability. In principle, the use of fugacity ratios as indicators of NAPL phase solubility limits can be extended to very complex systems such as coal tar, provided that the assumption of ideality in the NAPL phase holds.

NAPL/Aqueous Phase Equilibria. The results from the NAPL/aqueous phase equilibrium studies are tabulated in Tables 3 and 4. Table 4 lists measured and estimated aqueous phase concentrations. The estimated errors of the measured concentrations are typically less than 5%, but pyrene and fluoranthene concentrations have standard errors up to 20%. Notice that in NAPL 1, x_i^N for acenaphthene is very close to its solubility limit, resulting in an aqueous phase concentration very close to its pure solute aqueous solubility. The same is true for naphthalene in NAPL 2.

The estimated concentrations were computed using eq 4 assuming that $\gamma_i^N = 1$ and using the measured NAPL phase compositions for x_i^N values. A first-order uncertainty analysis was conducted to estimate uncertainty in the predicted values of C_i^A due to measurement error in x_i^N and uncertainty in the fugacity ratio and pure solute aqueous solubility. It was found that the largest contributor to error is the uncertainty in the fugacity ratio. Because of the multiplicative form of eq 4, the relative error in (f^s/f^l) translates directly into relative error in C_i^A. Thus, uncertainty in C_i^A predictions can be as large as 70%, as for pyrene. Again, the uncertainty increases as the system temperature becomes much smaller than the melting temperature, and thus is larger for the higher molecular weight PAHs.

The close agreement between the measured and estimated values of C_i^A indicates that the assumption of $\gamma_i^N = 1$ combined with available data to estimate the subcooled liquid solubility provides a reliable means of predicting aqueous concentrations in multicomponent NAPL/water systems. Deviations between measured and predicted values may indicate NAPL phase nonidealities or may simply reflect the inability to accurately estimate fugacity ratios.

These results demonstrate the utility of the synthetic NAPL materials for experiments to simulate PAH−NAPL contamination in aqueous environments. The formulations are sufficiently complex to result in stable liquefied PAH mixtures and to simulate the complex multicomponent NAPLs encountered as environmental contaminants, such as coal tars.

TABLE 4. Measurements of Aqueous Concentrations in NAPL/Water Phase Equilibrium Experiments

	C_i^A, concentration in aqueous phase (mg/L) with estimated error of $\pm 1\sigma$ (25 °C)							
	NAPL 1		NAPL 2		NAPL 3		NAPL 4	
compound	measd	estd[a]	measd	estd	measd	estd	measd	estd
toluene					10.7 (±0.4)	11	8.0 (±0.5)	9.5
naphthalene			29.4 (±0.7)	30			11.3 (±0.2)	12
1-methylnaphthalene	6.9 (±0.3)	6.0	7.3 (±0.3)	6.5	9.2 (±0.3)	8.4	8.0 (±0.1)	7.4
2-ethylnaphthalene	0.85 (±0.03)	0.75	0.51 (±0.04)	0.45	1.23 (±0.03)	1.2	1.07 (±0.01)	1.0
acenaphthene	3.5 (±0.2)	3.8	2.1 (±0.1)	2.3	2.5 (±0.1)	3.0	2.24 (±0.06)	2.6
fluorene	1.01 (±0.04)	1.0	0.66 (±0.05)	0.6	0.76 (±0.03)	0.8	0.67 (±0.03)	0.7
phenanthrene	0.73 (±0.03)	0.7	0.58 (±0.07)	0.4	0.57 (±0.02)	0.6	0.50 (±0.03)	0.5
fluoranthene	0.21 (±0.03)	0.2	0.24 (±0.05)	0.13	0.157 (±0.001)	0.16	0.16 (±0.01)	0.15
pyrene	0.08 (±0.02)	0.08	0.11 (±0.02)	0.05	0.071 (±0.001)	0.06	0.07 (±0.01)	0.05

[a] Estimated aqueous concentrations assuming ideality in the NAPL phase are shown for comparison.

Conversely, the mixtures are sufficiently simple to facilitate complete NAPL characterization, in terms of composition and bulk properties. This allows experimentation to simulate the dynamics of these characteristics with time such as may occur in natural or engineered environments. For example, the synthetic NAPLs have been used to measure mass transfer rates for NAPL dissolution (*6*) and the bioavailability of NAPL constituents in NAPL/aqueous phase systems.

Acknowledgments

This research was supported by Grant Project R-57 from the U.S. Environmental Protection Agency through the Northeast HSRC to Princeton University and by Grant ES04911 from the NIEHS Superfund Program to the University of Michigan. The authors also acknowledge Mr. E. Gung ('97) and Ms. G. Reynolds ('98), Princeton undergraduates who aided in experimental determinations of binary and ternary phase equilibria. Partial support for their activities was provided by a research award from the Alcoa Foundation.

Literature Cited

(1) Luthy, R. G.; Dzombak, D. A.; Peters, C. A.; Roy, S. B.; Ramaswami, A.; Nakles, D. V.; Nott, B. R. *Environ. Sci. Technol.* **1994**, *28*, 266A−276A.

(2) Hildebrand, J. H.; Scott, R. L. *The Solubility of Nonelectrolytes*, 3rd ed.; Reinhold Publishing Co.: New York, 1950; Chapter 17.

(3) Prausnitz, J. M.; Lichtenthaler, R. N.; de Azevedo, E. G. *Molecular Thermodynamics of Fluid-Phase Equilibria*, 2nd ed.; Prentice-Hall, Inc.: Englewood Cliffs, NJ, 1986; Chapter 9.

(4) Yalkowsky, S. H. *Ind. Eng. Chem. Fundam.* **1979**, *18* (2), 108−111.

(5) Mackay, D.; Shiu, W. Y.; Ma, K. C. *Illustrated Handbook of Physical-Chemical Properties and Environmental Fate for Organic Chemicals*; Lewis Publishers: Chelsea, MI, 1992.

(6) Mukherji, S.; Peters, C. A.; Weber, W. J., Jr. *Environ. Sci. Technol.* **1997**, *31* (2), 416−423.

(7) Rudolfi, E. *Z. Phys. Chem.* **1909**, *66*, 705−732.

(8) Peters, C. A.; Luthy, R. G. *Environ. Sci. Technol.* **1993**, *27* (13), 2831−2843.

(9) Leinonen, P. J.; Mackay, D. *Can. J. Chem. Eng.* **1973**, *51*, 230−233.

(10) Chiou, C. T.; Schmedding, D. W.; Manes, M. *Environ. Sci. Technol.* **1982**, *16*(1), 4−10.

(11) Banerjee, S. *Environ. Sci. Technol.* **1984**, *18*, 587−591.

(12) Burris, D. R.; MacIntyre, W. G. *Geochim. Cosmochim. Acta* **1986**, *50*, 1545−1549.

(13) Mackay, D.; Shiu, W. Y.; Maijanen, A.; Feenstra, S. *J. Contam. Hydrol.* **1991**, *8*, 23−42.

(14) Lane, W. F.; Loehr, R. C. *Environ. Sci. Technol.* **1992**, *26*, 983−990.

(15) Lee, L. S.; Hagwell, M.; Delfino, J. J.; Rao, P. S. C. *Environ. Sci. Technol.* **1992**, *26* (11), 2104−2110.

(16) Peters, C. A.; Labieniec, P. A.; Knightes, C. D. Multicomponent NAPL Composition Dynamics and Risk. *Proceedings of the ASCE Annual Convention, Conference: NAPLs in the Subsurface Environment: Assessment and Remediation*; ASCE: Washington, DC, Nov 1996; pp 681−692.

(17) Knightes, C. D.; Peters, C. A. Numerical Simulation of Multicomponent NAPL Dissolution and Precipitation. *WEFTEC'96*, Proceedings of the Water Environment Federation 69th Annual Conference, Dallas, TX; 1996; Vol. I, Part I, pp 333−343.

(18) *Chemical and Physical Characteristics of Tar Samples from Selected Manufactured Gas Plant (MGP) Sites*; EPRI TR-102184. Final report for research project 2879−12; Electric Power Research Institute: Palo Alto, CA, 1993.

(19) Daubert, T. E.; Danner. R. P. *Physical and Thermodynamic Properties of Pure Chemicals: Data Compilation*; Hemisphere Publishing Co.: New York, 1989.

(20) Morgan, M. G.; Henrion, M. *Uncertainty, A Guide to Dealing with Uncertainty in Quantitative Risk and Policy Analysis*; Cambridge University Press: New York, 1990; Chapter 8.

(21) Rhines, F. N. *Phase Diagrams in Metallurgy, Their Development and Application*; McGraw Hill: New York, 1956; Chapter 14.

Received for review November 11, 1996. Revised manuscript received April 22, 1997. Accepted April 24, 1997.[⊗]

ES960948M

[⊗] Abstract published in *Advance ACS Abstracts,* July 1, 1997.